Proceedings of FEDSM2007
5th Joint ASME/JSME Fluids Engineering Conference
July 30-August 2, 2007 San Diego, California USA

FEDSM2007-37382

CFD STUDY OF PROSPECTIVE 1ST STAGE CENTRIFUGAL IMPELLER DESIGN

Sergey S. Panaiotti
Moscow Bauman State Technical University
mgtu_ssp@elcomnet.ru

Upendra Singh Rohatgi
Brookhaven National Lab
rohatgi@bnl.gov

Sergey F. Timuchev
Moscow Aviation Institute
irico@mail.cnt.ru

Vladimir A. Soldatov
Russian Research Center "Kurchatov Institute"
soldatov@dhtp.kiae.ru

Boris N. Chumachenko
Keldysh Research Center
chumach@novotechnica.com

ABSTRACT

CFD analysis of two first - stage centrifugal impellers is undertaken with the main goal to obtain additional evaluation data regarding flow characteristics of the old first stage impeller design and in the proposed new cantilever impeller design. The new design is developed to reduce the 1st stage impeller cavitation erosion damage of a multistage centrifugal feed pump. This stage of work comprises computational tests of both impeller models under the same mode of operation, 3000 RPM and volumetric flow rate 0.0503 m3/s. Both impellers are planning to be tested experimentally. The inlet geometry for CFD tests is taken from the test facility draft. The outlet is made like a circular vaneless diffuser. In the old design, a hub developed upstream presents the through shaft. Computational results are compared with the head/efficiency data delivered by plane cascade theory. Computational data shows an advantage of the new design by head and efficiency although the efficiency level is underestimated. Computational data shows lower pressure zones in the proposed design are localized at the impeller inlet periphery, in the old design lower pressure zones spreads along the blade inlet height. Further computational test will be made for the whole geometry including the stage stator part and experimental validation of the proposed design will follow.

INTRODUCTION

The multistage centrifugal pumps are applied as feed pumps in heat and nuclear power plants, in ship energy installations, in petroleum and other industries. Such pump has a long through shaft of large diameter with two tip shaft seals, oil lubrication bearings installed beyond the pump casing, and a lateral fluid inlet to the first stage. The long through shaft worsens the rotor dynamics, increases fluid velocity at the impeller inlet reducing cavitation quality, and strengthens cavitation erosion of the pump first stage. Despite of disadvantages, such design concept of multistage centrifugal feed, petroleum, mine and other pumps is conventional.

During activity under the CRDF contract in the pump laboratory of Kaluga branch of Bauman Moscow State Technical University (Bauman MSTU) a preliminary design of the new multistage feed pump for 300 MW power unit is developed. It has the first stage cantilevered impeller and axial fluid inlet. The pump shaft rotates in two hydrodynamic bearings fed by the pumping fluid. The first bearing bush is located in the vane stator disk bore, and the second - before the unique tip shaft seal at the pump drive side. The indicated arrangement of bearings allows to reduce essentially the shaft length and its bend and to improve dynamics characteristics. Cantilever centrifugal impeller installation of the first stage decreases input diameter and relative flow velocity at the blade input. It improves suction capability and decreases cavitation erosion intensity. In the laboratory pump old and new model of the multistage feed pump first stage will be tested. Confuser inlet, centrifugal impellers and vane diffuser with return channels are designed by one-dimensional theory developed in Bauman MSTU.

With rotation speed $n = 3000 RPM$ and flow rate $Q = 0.05\ m^3 / s$ both stages are designed for a head level of $H = 69\ m$. The stage specific speed makes $n_S = 3.65 \cdot n \cdot \sqrt{Q} / H^{0.75} = 100$, cavitation specific speed is $C = 5.62 \cdot n \cdot \sqrt{Q} / NPSH^{0.75} \approx 1000$ and reduced eye diameter coefficient $K_0 = \sqrt{D_0^2 - d_h^2} / \sqrt[3]{Q / n} \approx 3.9$ that is typical for the modern feed pump first stage. Both centrifugal impellers are

contoured by conformal mappings method. Blades have cylindrical form at the exit and spatial shape at the impeller inlet. The latter gives small positive angles of attack and avoids flow separation and back flow at the impeller inlet. The ratio of inlet diameters of old and new impeller designs makes 1.4. The intensity of cavitation erosion is proportional about the sixth power of the ratio of input peripheral velocities [1, 2]. Thus, one can expect that with the cantilever impeller the intensity of cavitation erosion will decrease approximately by a factor of 8. The methods planned to be used for evaluation of the cavitation erosion include location of varnish coating removal, forms of the cavities, length of the cavities, and vibrations and pressure pulsations level. CFD unsteady flow analysis is undertaken to get additional evaluation data regarding flow parameters of two impeller designs. The part of this computational procedure[3, 4, 5] is a common iterative method for non-compressible fluid flow.

NOMENCLATURE

$\mathbf{V}$ -- Velocity vector
t -- Time
x -- spatial coordinate
P -- Relative static pressure
ρ -- Density
μ -- Dynamic viscosity
$\mathbf{F}$ -- Volumetric force
k -- Turbulence energy
ε -- Turbulence dissipation rate

GOVERNING EQUATIONS

The mathematical model bases on the Navier-Stokes equations

$$\frac{\partial \mathbf{V}}{\partial t} + \nabla(\mathbf{V} \otimes \mathbf{V}) = -\frac{\nabla P}{\rho} + \frac{1}{\rho}\nabla((\mu + \mu_t)(\nabla \mathbf{V} + (\nabla \mathbf{V})^T) + \mathbf{F} \quad (1)$$

and taking into account the continuity equation for incompressible liquid

$$\nabla \mathbf{V} = 0 \quad (2)$$

Relation (3) uses standard $k-\varepsilon$ model of turbulence [6] to determine turbulent viscosity

$$\mu_t = C_\mu \rho \frac{k^2}{\varepsilon} \quad (3)$$

The following equations make kinetic energy and dissipation:

$$\frac{\partial k}{\partial t} + \nabla(\mathbf{V}k) = \frac{1}{\rho}\nabla((\mu + \frac{\mu_t}{\sigma_k})\nabla k) + \frac{G}{\rho} - \varepsilon \quad (4)$$

$$\frac{\partial \varepsilon}{\partial t} + \nabla(\mathbf{V}\varepsilon) = \frac{1}{\rho}\nabla((\mu + \frac{\mu_t}{\sigma_\varepsilon})\nabla \varepsilon) + \frac{\varepsilon}{k}(C_1 \frac{G}{\rho} - C_2 \varepsilon) \quad (5)$$

Where $G = \mu_t \frac{\partial V_i}{\partial x_j}(\frac{\partial V_i}{\partial x_j} + \frac{\partial V_j}{\partial x_i})$

The turbulence model constants are

σ_k =1.0; σ_ε =1.3; C_μ =0.09; C_1 =1.44; C_2 =1.92

Navier-Stokes equations are solved by splitting method with implicit algorithm and high-order numerical scheme for convective transfer terms. Initial condition is zero pressure and velocity in entire computational domain. Initial values of kinetic energy and dissipation are calculated automatically during the first step of computation. At the inlet boundary the normal velocity component defines volumetric flow rate. At the outer boundary, free-outlet flow condition is used with constant pressure and linear extrapolation of velocity from inner nodes.

Boundary condition on the wall represents a logarithmic law numerical equivalent for the velocity tangential component. It makes from the following expression

$$\frac{V_\tau}{V_*} = \begin{cases} y^+, & y^+ < y_*^+ \\ u^+ & y^+ \geq y_*^+ \end{cases} \quad (6)$$

$$V_* = \sqrt{\frac{\tau_w}{\rho}} \ ,$$

where V_* is the friction velocity, τ_w is the wall shear stress and the turbulent boundary layer kinematical parameters are defined by the following formulas

$$u^+ = \frac{1}{\kappa}\ln(Ey^+) \quad (7)$$

$$y^+ = \frac{\rho V_* h}{\mu} \quad (8)$$

where $\kappa = 0.4$, $E = 10$, $y_*^+ = 11.96$ and h makes a distance from the wall to the center of the boundary grid cell.

COMPUTATIONAL PROCEDURE

Computational Domain

The computational domain is divided on 3 parts – inlet, rotor and stator. The inlet and stator (outlet) are motionless parts. They link to the rotor part by "sliding-grid" interface accounting rotation of the impeller. It makes an interpolation of flow data from motionless part to rotating part and vise-versa accounting impeller rotation speed. Computational domains for two impeller designs are presented in *Fig. 1* and. In computational space, three above-mentioned domains shift from actual positions and link virtually to each other through sliding surfaces at the impeller inlet and outlet. These sliding interfaces serve as control surfaces in estimation impeller characteristics. In the old design, a hub developed upstream presents the through shaft. The part of the hub locates in the inlet motionless domain. The rotation of this part is accounted

by a velocity-swirl boundary condition that ensues adequate modeling of the experimental test condition.

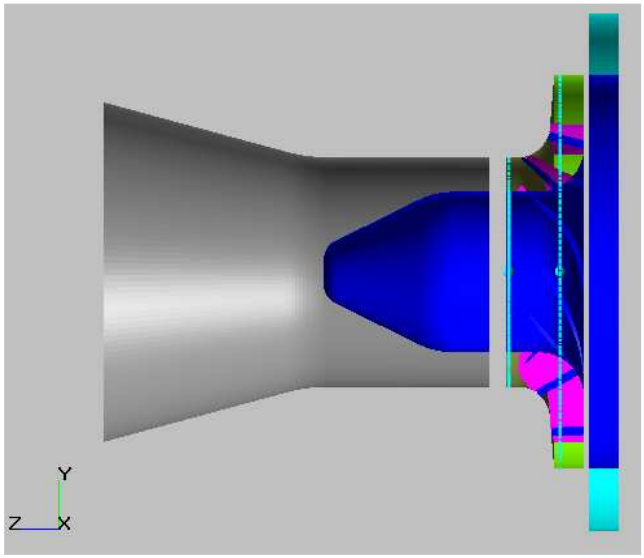

Fig. 1: Old design with through shaft simulation

Computational Grid

The 3D numerical procedure bases on non-staggered Cartesian grid with adaptive local refinement and a sub-grid geometry resolution method for description of curvilinear complex boundaries.

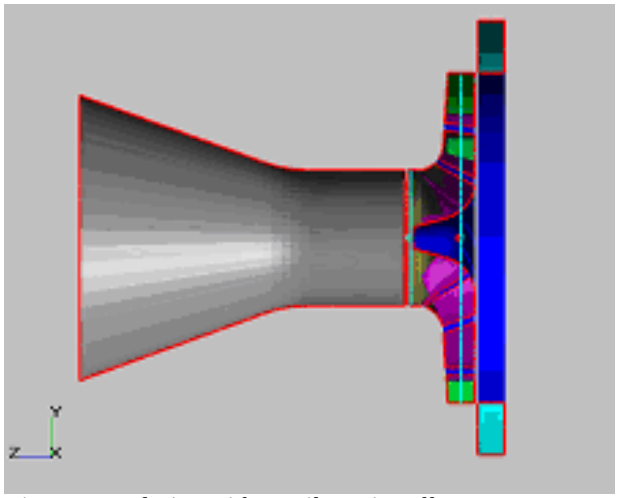

Fig. 2: New design with cantilever impeller

During grid adaptation, an initial grid can be made denser by splitting each parent grid cell to 8 smaller cells near wall boundaries with new adaptation level. In addition, grid cells intersected by wall makes polyhedron cells keeping real geometrical parameters and improving accuracy even with a relatively lower total number of cells.

The grid adaptation method gives reduction in overall processor time by making computation on a rough grid during first 6 impeller turns. Then the grid refines when approaching to the convergent oscillatory solution. Present computational tests are completed on grids of 200-400 thousand cells for both impeller designs. Sketches of the computational grid adapted near wall and blade surfaces are presented in *Fig. 3* for the new impeller design inlet view and *Fig. 4* for the meridional view. On blade surfaces the 3rd level of grid adaptation, in the inlet and outlet sliding surfaces the 2nd level of grid adaptation. is applied.

Such a grid provides on blade wall surface the turbulent layer kinematical parameters giving $30 \le y^+ \le 300$ by relation (8).

Convergence and Post-Processing

Iterative procedure goes up to convergence to a "steady" periodical solution. Resulting impeller flow characteristic parameters can be determined by time- and flow-averaging of unsteady computational flow data. The convergence is controlled by the effective head value level between inlet and outlet rotor sliding surfaces. One determines it from a differential of time- and flow-averaged total pressures through the inlet and outlet sections of the impeller

$$H = (P_{02} - P_{01}) / \rho .$$

One has to note the pressure reference level is 101000Pa. In computations and resulting data, one makes pressure values from the reference level and it delivers negative inlet static and total pressure values.

Theoretical head comes from Euler relation by time- and flow-averaged circumferential and circular velocity components

$$H_t = C_{u2} \cdot U_2 - C_{u1} \cdot U_1 .$$

Finally, the impeller hydraulic efficiency makes from ratio of the effective and theoretical head

$$\eta = H / H_t .$$

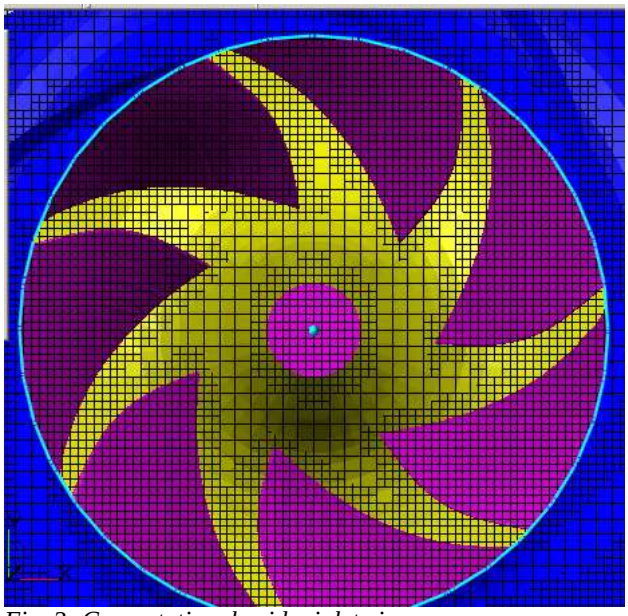

Fig. 3: Computational grid – inlet view

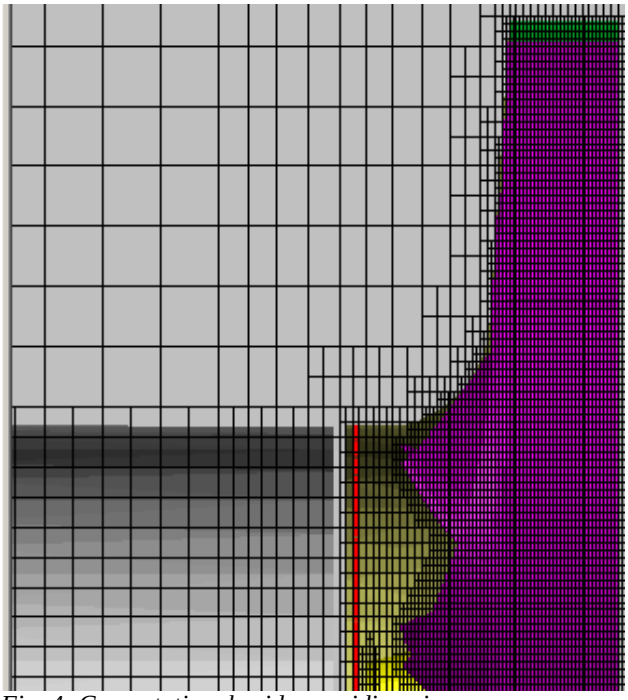

Fig. 4: Computational grid – meridian view

COMPUTATIONAL RESULTS

Computations are completed on double Pentium – IV processor PC with 2 Gb RAM. Computational results for the new impeller are outlined below. There are presented instantaneous flow parameters distributions for the new impeller design. Anyway one can say the old design has qualitatively the same flow parameters behavior.

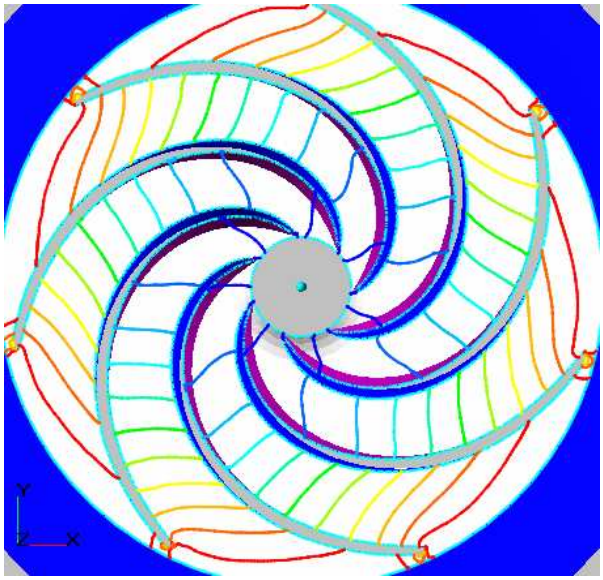

Fig. 5: Static pressure isolines in the new impeller design; deep blue color stands for -600000 Pa, red color stands for -100000 Pa

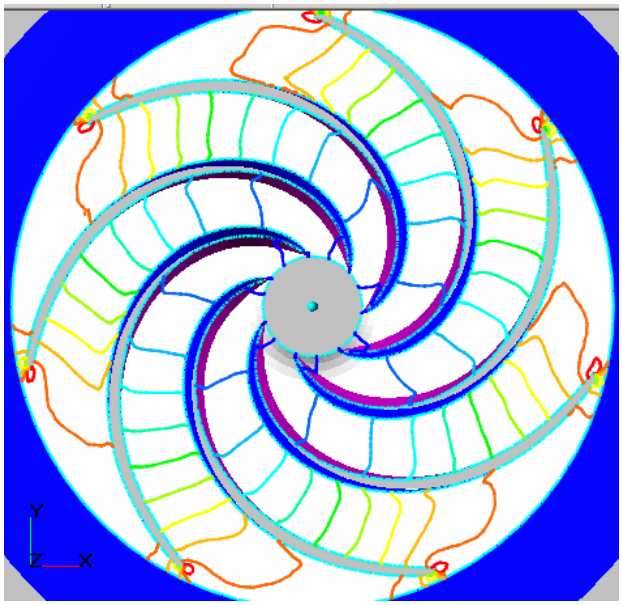

Fig. 6: Total pressure isolines in the new impeller design; deep blue color stands for -600000 Pa, red color stands for 200000 Pa

In Fig. 5 and Fig.6, one can find distribution of static and total pressure in the cantilever impeller design. It shows the impeller flow has a steady character with a constant smooth increasing of fluid energy downstream. The only distortions of flow one can note at blade tips. The same conclusion one can make on absolute and relative vector maps shown in Fig. 7 and Fig. 8. There are no flow separations or back flow zones in the blade channels. The same data are obtained for the old design with through shaft. This ensures both impeller designs near the best efficiency point have no essential flow distortions that spoil energetic characteristics.

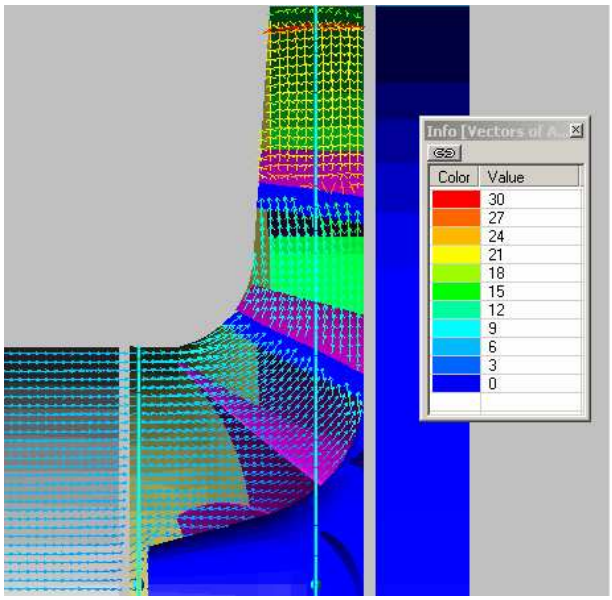

Fig. 7: Absolute velocity vectors in the new impeller design

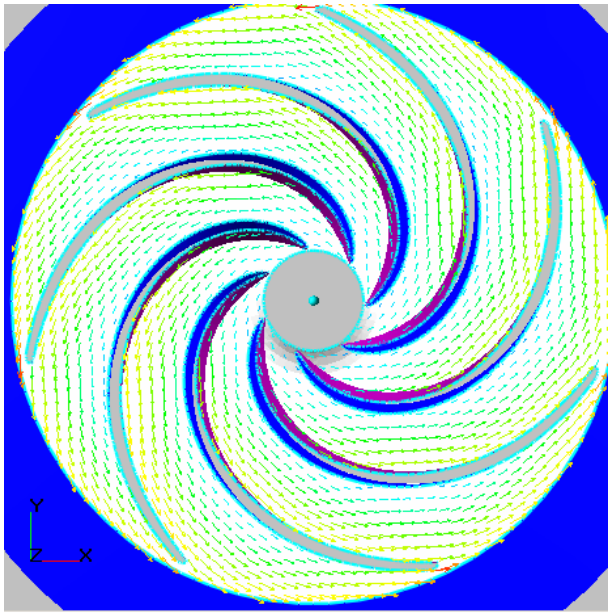

Fig. 8 Relative velocity vectors in the new impeller design

In *Fig. 9* and *Fig. 10* are presented surfaces of instantaneous static pressure level –650000Pa for the old and new impeller design. One can note the lower pressure zones in the new design are at the impeller inlet periphery, in the old design lower pressure zones spreads along the blade height.

This shows the through shaft can provoke a more extensive impeller cavitation erosion but this result needs additional study with application of denser grid by using parallel computations.

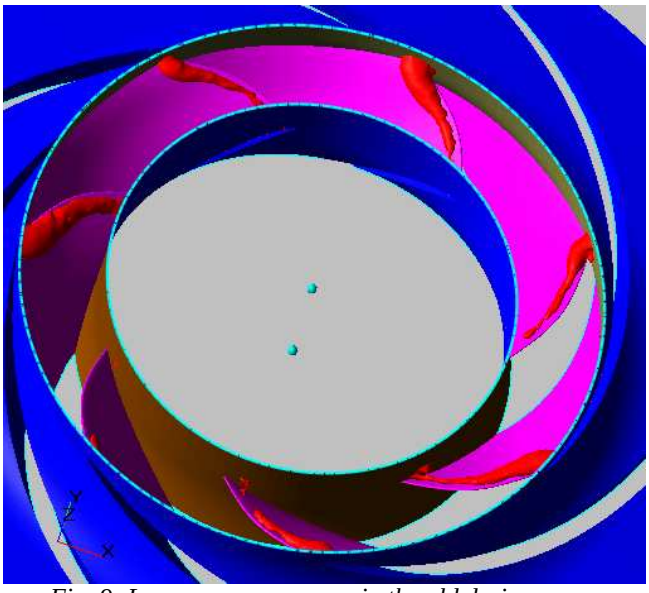

Fig. 9: Lower pressure zones in the old design

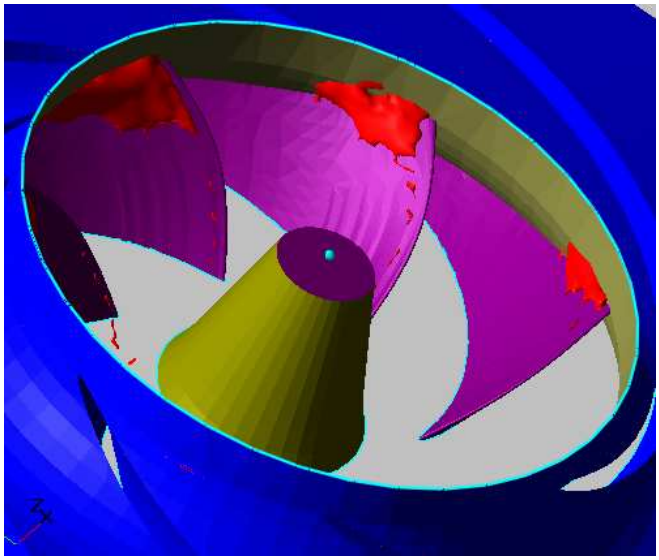

Fig. 10: Lower pressure zone in the new design

Below are outlined impeller design characteristic data. They show better parameters for the cantilever impeller design although the absolute efficiency value is underestimated. The plane cascade theory calculations gives theoretical head values 780 – 797 J/kG.

Parameter	Old design	New design
Ht [J/kG]	775	800.37
H [J/kG]	726.13	762.8
Efficiency	0.9369	0.9531

ACKNOWLEDGEMENTS

The authors will like acknowledge the support of Flowserve and grant from Initiative for Proliferation Prevention program of Department of Energy (CRDF #10231).

REFERENCES

[1] Gulich J.E. Guidelines for Prevention of Cavitation in Centrifugal Feed Pumps//EPRI GS — 6398, November, 1989.

[2] Visser F.C., Backx J.J.M., Greets T., Cugal M., Miguel D. Pump Impeller lifetime Improvement through Visual Study of Leading-Edge Cavitation. Proceedings of the fifteenth International Pump User Symposium Turbomachinery Laboratory, Texas A@M University, College Station, Texas, USA, 1998. — P. 109–117.

[3] Serguei Timouchev. FEDSM2005-77354 Computational study of pressure pulsation in a medium specific speed pump. Proceedings of FEDSM2005: 2005 ASME Fluids Engineering Division Summer Meeting and Exhibition June 19-23, 2005, Houston, TX, USA

[4] A. Aksenov., A. Dyadkin., A. Gudzovsky . Numerical Simulation of Car Tire Aquaplaning. Computational Fluid Dynamics '96, J.-A. Desideri, C.Hirsch, P.Le Tallec, M.Pandolfi, J.Periaux edts, John Wiley&Sons, pp. 815-820, 1996

[5] Serguei Timouchev, Andrey Aksenov, Victor Bogdanov, Alexander Karpyshev. FEDSM2005-77355 Computational study of ejector-pumps Proceedings of FEDSM2005: 2005 ASME Fluids Engineering Division Summer Meeting and Exhibition June 19-23, 2005, Houston, TX, USA

[6] Wilcox, D. C. Turbulence modeling for CFD, DCW Industries, Inc., 460 p, 1994